Geophysical Research Letters

Supporting Information for

Melting Experiments on Fe-O-H and Fe-H: Evidence for Eutectic Melting in Fe-FeH and Implications for Hydrogen in the Core

Kenta Oka[1], Nagi Ikuta[1], Shoh Tagawa[1,2], Kei Hirose[1,2], and Yasuo Ohishi[3]

[1]Department of Earth and Planetary Science, The University of Tokyo, Bunkyo, Tokyo, Japan

[2]Earth-Life Science Institute, Tokyo Institute of Technology, Meguro, Tokyo, Japan

[3]Japan Synchrotron Radiation Research Institute, SPring-8, Sayo, Hyogo, Japan

Contents of this file

Experimental Methods

Melting experiments on the Fe-O-H system. We used diamond anvils with flat 300 μm or single-beveled 120 μm culet size for experiments on Fe-O±H (Table S1). A pure Fe (5N, *Mairon-UHP*, *Toho Zinc*) or Fe-12wt%O foil, same as that used in Oka et al. (2019), was loaded into a hole at the center of a pre-indented rhenium gasket, together with a powder mixture of $Al(OH)_3$ and Al_2O_3 (a source of oxygen and hydrogen) and 10 μm-thick Al_2O_3 sapphire single crystals (thermal insulation layers). Upon heating, $Al(OH)_3$ dehydrates to form AlOOH or Al_2O_3. The mixing ratio between Al_2O_3 and $Al(OH)_3$ was varied in order to change the Fe/H_2O ratio of a system.

The sample was heated from both sides with a couple of 100W single-mode Yb fiber lasers with flat-top beam-shaping optics. The laser spot size was 20–30 μm across. The heating duration was limited to less than 3 sec to avoid temperature fluctuations which could lead to a complex melting texture. Indeed, it is long enough for O and H to diffuse over a melt pocket (Helffrich, 2014), which assures chemical equilibrium between liquid and solid when considering that melting/crystallization at the liquid-solid boundary occurs almost instantaneously (Yokoo et al., 2019; Hasegawa et al., 2021). According to previous time-series melting experiments on the Fe-S system, the compositions of coexisting liquid and solid did not change after heating for 1 sec in a laser-heated DAC (Mori et al., 2017). The diffusivities of O and H in molten iron are higher than that of S (Helffrich, 2014). A temperature profile was obtained using a spectro-radiometric method (Hirao et al., 2020). The temperature at the liquid/solid boundary corresponds to the liquidus temperature of a liquid obtained in each run. We determined it by combining the temperature profile with a sample cross-section (e.g., Mori et al., 2017; Tateno et al., 2018; Oka et al., 2019) (Figure 2c).

We performed XRD measurements in-situ at high *P*-*T* using an X-ray beam with energy of ~30 keV at the beamline BL10XU, SPring-8 (Figure 1). XRD spectra were collected on a flat panel detector (FPD, *Perkin Elmer*) with exposure time of 1 sec before and after heating at 300 K and of 0.2 sec continuously during laser heating. The IPAnalyzer software (Seto et al., 2010) was used to integrate two-dimensional XRD image into one-dimensional diffraction profile. Sample pressure was measured at 300 K after heating based on the unit-cell volume of Al_2O_3 corundum and its equation of state (Dewaele & Torrent, 2013). We considered that 60% and 90% of theoretical thermal pressure for purely isochoric heating, $\Delta P = \alpha K_T \times (T - 300)$ ($\alpha K_T = 4$ and 9 MPa/K), contributed to an increase in sample pressure during heating at ~40 GPa and ~150 GPa, respectively (e.g., Hirose et al., 2019; Oka et al., 2019).

Textural and chemical characterizations except for H (see below) were carried out on each recovered sample; it is well known that H escapes from metal Fe when it transforms into bcc during decompression (e.g., Iizuka-Oku et al., 2017; Tagawa et al., 2021). A sample cross-section and X-ray elemental maps were obtained parallel to the compression axis by a focused ion beam (FIB, *FEI Versa 3D DualBeam*) and an energy-dispersive spectroscopy (EDS) attached to a field-emission (FE)-type scanning electron microscope (SEM) (Figures 2a, b). Quantitative chemical analyses were then made for coexisting liquid and crystals (liquidus phases) with an FE-type electron probe micro-analyzer (FE-EPMA, *JEOL JXA-8530F*) with an accelerating voltage of 12 kV, a current of 15 nA, and the X-ray counting time of 20/10 sec for peak/background. Fe, Fe_3C, and corundum were used as standards. LIF (Fe), LDE2H (C), TAP (Al), and LDE1 (O) were analyzing crystals. The FE-EPMA analyses of quenched liquid Fe sometimes included a small amount of Al, which is likely a signal from the surrounding pressure medium or Al_2O_3 grains that mechanically intruded into the liquid; note that the amount of Al incorporated into liquid Fe metal is negligible (Badro et al., 2016; Helffrich et al., 2020). Al was therefore subtracted as Al_2O_3 from raw data. C was detected not only in the quenched liquid but also inside the rhenium gasket; the latter could be due to contamination during FIB and/or FE-EPMA analysis. Thus, we subtracted 0.2–0.4 wt% C from the raw analyses of liquids, which was found on the rhenium gasket in the same sample cross-section. The liquid should have included the remaining 0.1–3.7 wt% C (Table S1).

H concentration, x in FeH_x, was estimated from its lattice volume (Hirose et al., 2019; Tagawa et al., 2021), which expands proportionally to the H content (Caracas, 2015);

$$x = \frac{V_{FeHx} - V_{Fe}}{\Delta V_H}, \quad (1)$$

where V_{FeHx} and V_{Fe} are the unit-cell volumes of FeH_x and Fe (Dorogokupets et al., 2017 for fcc Fe and Dewaele et al., 2006 for hcp Fe), respectively, and ΔV_H is an increase in the lattice volume of Fe per H atom from Caracas (2015). Note that theoretically-derived ΔV_H for the hcp phase at 0 K by Caracas (2015) is quite consistent with the room-temperature ΔV_H obtained experimentally for fcc by Tagawa, Gomi et al. (2022). The error in the H content, x, is estimated to be ±8% at maximum, which is mainly derived from uncertainty in ΔV_H (Ikuta et al., 2019; Tagawa et al., 2021).

Melting experiment on the Fe-H system. We have also conducted a melting experiment on the Fe-FeH binary system (Table S2), using a laser-heated DAC with beveled 200 μm culet anvil. A 10-μm thick pure iron foil was loaded between the pellets

of Al_2O_3 powder. A whole DAC was dried in a vacuum oven at 393 K for at least 1 hr and subsequently at 350 K for 30 min in a vacuumed hydrogen-loading system.

Hydrogen was cryogenically loaded into a sample chamber (Chi et al., 2011). After the chamber was filled with liquid hydrogen, sample was compressed at ~15 K and then restored to room temperature. The surface of the diamond anvils was coated with a thin layer of Ti by sputtering (Ohta et al., 2015) in order to avoid anvil failure. We synthesized the FeH_x sample at 10 GPa and melted it at 45 GPa with in-situ XRD measurements at BL10XU, SPring-8 (Figure 1b). We obtained pressures from the Raman shift of a diamond anvil (Akahama & Kawamura, 2004) and from the lattice volume of Al_2O_3 corundum when XRD data were available (Dewaele & Torrent, 2013). The temperature at the liquid/solid boundary was found to be 1900 K in the temperature profile considering the width of a liquid pool estimated by scanning the sample with respect to an X-ray beam. Other procedures including the determination of the H contents in solid and liquid Fe phases were similar to those for the Fe-O±H sample described above.

Table S1

Experimental Results on the Fe-O±H System

Run #	Starting materials	P (GPa) at high T	P (GPa) at 300 K	T (K)	Liquid composition			Liquidus phase
					O (wt%)	H (wt%)	C (wt%)	
A1	Fe-12wt%O + Al_2O_3 + $Al(OH)_3$[a]	35(2)	30(2)	2460(120)	3.53(4)	0.27(2)	1.68(9)	FeO
A2	Fe-12wt%O + Al_2O_3 + $Al(OH)_3$[b]	37(2)	32(2)	2470(110)	7.20(4)	0.18(1)	0.11(9)	FeO
A3	Fe-12wt%O + Al_2O_3 + $Al(OH)_3$[b]	41(2)	36(2)	2400(120)	9.53(18)	0.22(2)	0.20(12)	FeO
A4	Fe + $Al(OH)_3$	39(2)	33(2)	2370(120)	2.98(29)	0.49(4)	0.43(4)	Fe[d] + FeO
A5	Fe + Al_2O_3 + $Al(OH)_3$[c]	147(15)	122(12)	3200(320)	12.97(86)	0.00(0)	0.86(7)	Fe
A6	Fe + Al_2O_3 + $Al(OH)_3$[c]	160(16)	136(14)	3200(320)	10.36(56)	0.04(0)	3.74(23)	FeO

[a] Al_2O_3 : $Al(OH)_3$ = 10 : 3 by weight

[b] Al_2O_3 : $Al(OH)_3$ = 10 : 4 by weight

[c] Al_2O_3 : $Al(OH)_3$ = 10 : 8 by weight

[d] contains 0.43(3) wt% H calculated from its unit-cell volume of 20.5 $Å^3$

Table S2

Experimental Results on the Fe-H System

Run #	P (GPa)	T (K)	solid hcp-FeHx				quenched liquid hcp-FeHx			
			a (Å)	c (Å)	V ($Å^3$)	x	a (Å)	c (Å)	V ($Å^3$)	x
B	10(1)	300	2.528(1)	4.067(3)	22.51(8)	0.30(2)				
	45(2)	1900(100)	2.426(5)	3.969(7)	20.23(24)					
	41(2)	300	2.422(0)	3.894(1)	19.78(3)	0.20(2)	2.418(2)	3.948(5)	20.00(13)	0.26(2)

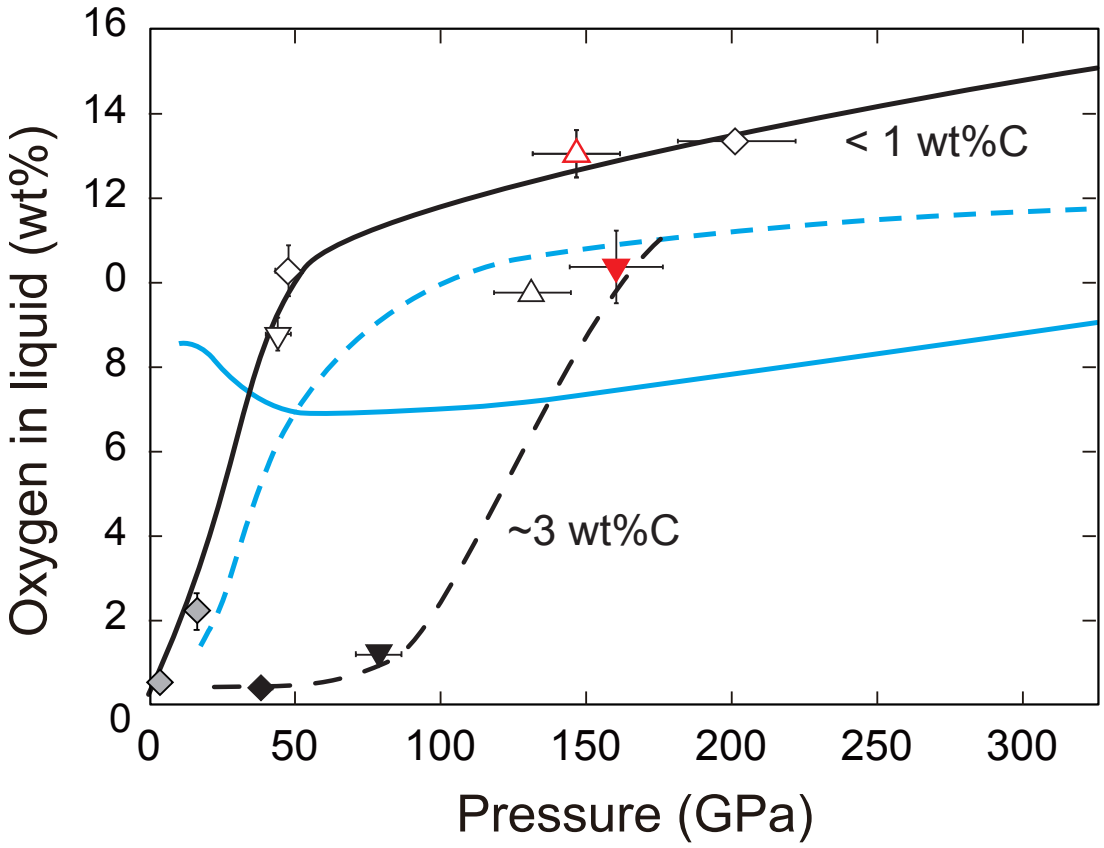

Figure S1. Liquid compositions obtained in melting experiments on the Fe-FeO±C system. Normal and reverse triangles, lower and upper bounds for O concentration in the Fe-FeO eutectic liquid, respectively; diamonds, the O contents in liquids coexisting both Fe and FeO (eutectic liquids). Red, this study (runs #A5 and #A6); black, Oka et al. (2019); gray, Ohtani et al. (1984) and Ringwood & Hibberson (1990). The black curves indicate changes in O concentration in liquids coexisting with Fe and FeO (solid line, with <1 wt% C in liquids; broken line, with ~3 wt% C in liquids). Blue dashed and solid curves represent thermodynamically-modelled eutectic liquid compositions in the Fe-FeO system assuming non-ideal and ideal solutions, respectively (Komabayashi, 2014).